Crossover in the adsorption properties of alkali metals on graphene

Kyung-Hwan Jin,[1] Seon-Myeong Choi,[1] and Seung-Hoon Jhi[1,2,*]
[1]*Department of Physics, Pohang University of Science and Technology, Pohang 790-784, Korea*
[2]*Division of Advanced Materials Science, Pohang University of Science and Technology, Pohang 790-784, Korea*
(Received 21 April 2010; published 30 July 2010)

The adsorption of alkali metals (AMs) on single layer graphene is studied using first principles methods. We observe a common trend in the binding distance, the charge transfer, and the work function (W) at certain coverage of AMs with increase in the proportion ρ (adatom/C atom) of the graphene covered by the AM. A dip in these properties occurs at $\rho \approx 0.04$ for all AMs except Li, for which it occurs at $\rho \approx 0.08$. This behavior is due to a transition of adsorbed metals from individual atoms to two-dimensional metallic sheets that exert a depolarization effect. W of graphene exhibits asymmetric dependence on ρ: a dip in the adatom layer side but saturation on the graphene side, which is in contrast to the case of bulk graphite.

DOI: 10.1103/PhysRevB.82.033414 PACS number(s): 73.22.Pr, 68.43.Bc, 73.20.Hb

INTRODUCTION

Graphene is a one atom thick, truly two-dimensional (2D) carbon material that exhibits many intriguing electronic properties such as massless Dirac-fermion-like charge carriers and quantum Hall effects.[1–3] This material has potential applications in nanoelectronic devices and also is considered for use as a supporting template for catalytic metal particles and for energy storage.[4,5] Controlling graphene's characteristics to make it useful for practical applications has been extensively explored.[6,7]

Chemical doping and making a good contact with metal electrodes are key issues that need comprehensive understanding for device applications. Alkali metals (AMs) and alkaline earth metals adhere nondestructively to graphene, and allow it to retain its electronic properties.[6,8–10] These metals become bonded ionically with graphene by donating electrons, which then become delocalized. The edge-localized electrons in graphene nanoribbons, lead to unusual self-assembled atomic wires at the zigzag carbon edges.[9] Studies on intercalation of these metals in graphite have been conducted,[11,12] but the process has not been well characterized on single layer graphene. The adsorbed metal atoms start interacting with each other when their coverage exceeds certain values; ultimately, they will form a 2D metallic sheet. The ionic radii may be a gauge of the onset of such interactions.

In this paper, we use the pseudopotential density functional method to characterize how the electronic properties of graphene with adsorbed AMs change as ρ changes. AMs donate one electron to graphene, which increases the Fermi level and thus reduces the work function W of the graphene without altering the massless Dirac fermionlike nature of the graphene band structure.[6,10] Studies of the intercalation of AMs in graphite have been conducted to observe the stages and phases of intercalated metal atoms.[11,13] The bounding graphite layers impose a constraining force on the intercalated metals. In contrast, the metals on a single graphene layer are free to migrate, and the interactions between metal atoms can have a truly 2D character. We explore the adsorption behavior of the metal and its influence on the electrical properties of graphene.

COMPUTATIONAL METHODS

We conducted first principles calculations based on the pseudopotential density functional method as implemented in the Vienna ab-initio simulation package (VASP).[14] The exchange correlation of electrons was treated within the local spin density approximation.[15,16] The cutoff energy for the expansion of wave functions and potentials in the plane-wave basis was chosen to be 400 eV, and the Brillouin zone sampling was done using the Monkhorst-Pack special k-point method with a grid of $15 \times 15 \times 1$ for the 2×2 phase or with equivalent number of k points. The atomic relaxation was continued until the Helmann-Feynman forces were less than 0.02 eV/Å. The vacuum layer in the supercell used in our calculations is set to be 15 Å, which is enough to minimize the artificial interlayer interactions.

The adatom-graphene system at various coverage was modeled by putting one metal adatom on 2×2, $\sqrt{7} \times \sqrt{7}$, 3×3, 4×4, 5×5, and 6×6 hexagonal graphene supercells. These configurations correspond to $\rho = 1/8$, 1/14, 1/18, 1/32, 1/50, and 1/72 adatom/C, respectively. Although each metal has a different maximum ρ, we chose this convention to study the coverage dependence of the adsorption properties of different metals on equal footings. Adatom-graphene structures typically develop rhomboid unit cells (Fig. 1). We considered AM adsorption on a single side of graphene because graphene is in most cases deposited or grown on substrates. The adsorption on both sides may be possible for suspended graphene, but our calculations showed that the binding energy for two Na atoms on both sides of graphene (one Na on each side) is smaller than that for two Na atoms

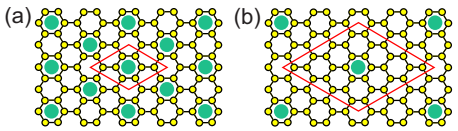

FIG. 1. (Color online) Schematic atomic structure of alkali metal-adsorbed graphene. Adatoms in hollow sites on graphene in (a) 2×2 and (b) 4×4 supercell structure. Green (large gray) circles: alkali metal atoms; yellow (small gray) circles: carbon atoms; red parallelograms: unit cells.

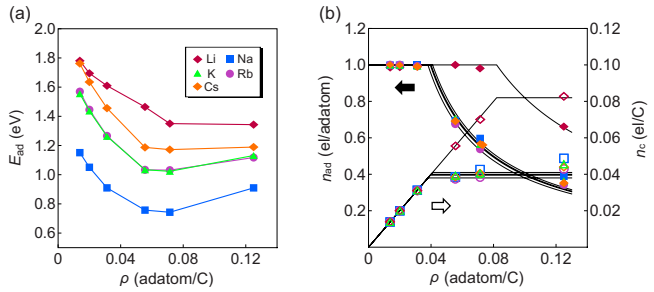

FIG. 2. (Color online) (a) Calculated binding energy E_{ad} of AMs on graphene at varying adatom coverages (ρ, adatom/C) and (b) charge transfer from adatom to graphene per adatom (n_{ad}, filled data points) or per carbon atom (n_c, open data points). The curves of $1/\rho$ for n_{ad} in (b) are the analytic form obtained by minimizing the adsorption energy with respect to the coverage (see the text). For Li, the trends of E_{ad} and charge transfer (n_{ad} and n_c) over ρ differ from those of the other AMs.

on the same side of graphene (by 0.04 eV). Thus, at early stages, Na will start adsorbing on the same side at low temperatures.

RESULTS AND DISCUSSIONS

The adsorption energy E_{ad}, the charge transfer n_{ad} (electrons/adatom) (or n_c in electrons/C-atom unit) from metal to graphene, effective adsorption distance d_{eff}, and W of graphene were calculated as ρ increased. E_{ad} was calculated incrementally; $E_{ad}=E_t[\text{graphene}+\text{nM}]-E_t[\text{graphene}+(\text{n}-1)\text{M}]-E_t[\text{M}]$ where $E_t[\cdot]$ is the total energy of the system $(\cdot)$. W was given as the energy from the Fermi level to the vacuum level, which is set to be the average potential energy far from the graphene surface.[17] In order to remove the slowly converging dipole field, we calculated the potential energy in the middle of two identical but inverted AM-adsorbed graphene layers that are separated by 15 Å. The d_{eff} is the adsorption distance minus the ionic radii of adsorbed metals.[18] These properties showed a strong dependence on ρ, which was incorporated into a model that considers the graphene electronic structure and the Coulomb interaction of adatom-graphene and adatom-adatom.

For single atom adsorption, the hollow sites were found to be more favorable than carbon bridge or top of carbon atoms for all AMs.[19] This result was the same even when ρ was changed. Calculated adsorption energy E_{ad} and charge transfer n_{ad} (or n_c) for AMs at various coverages (Fig. 2) were in reasonable agreement with other calculations.[20,21] We observe a weak parabolic behavior of E_{ad} as ρ increased [Fig. 2(a)]. The decrease of E_{ad} at low ρ is due to the increase in the Fermi energy of graphene by electron transfer, but adatoms became more closely packed and started to form metallic bonds with each other at higher ρ leading to the increase in the adsorption energy resultantly. For ionically bonded adatoms, E_{ad} and the charge transfer results from a balance of the electronic energy of the electrons transferred to graphene and the Coulomb interaction between the oppositely charged adatom and surface and the short-range electron repulsion.

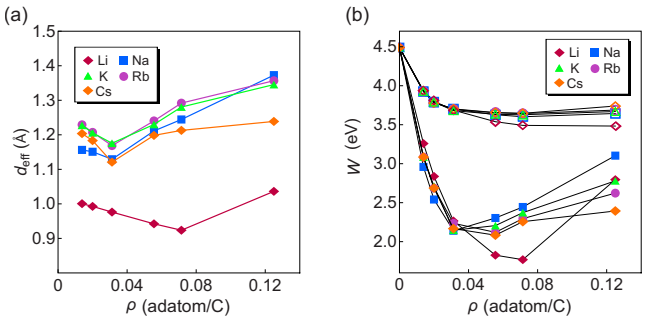

FIG. 3. (Color online) (a) Calculated effective binding distance d_{eff} and (b) work functions (W) of adatom-graphene systems. d_{eff} was obtained by subtracting the ionic radii of the metal from the calculated adsorption distance. In (b), filled points denote the calculated W on the adatom side, and open points denote calculated W on the graphene layer side. W for AMs except Li decreased with increasing ρ along a common curve to a minimum at $\rho \approx 0.04$, but for Li it continued to decrease to a minimum at $\rho \approx 0.08$.

The electronic structure of graphene is not altered by metal adsorption, so a straightforward way to calculate charge transfer is to integrate graphene's density of state from the Dirac point to the Fermi level. At low ρ, the s electron of AM is completely transferred to graphene, and n_{ad} decrease as the inverse of ρ after ρ exceeds a certain value. This $1/\rho$ behavior is obtained by maximizing the energy gain from the transfer, which is expressed as $E_{ad}=an-b\rho^{1/2}n^{3/2}+cn^2\rho$, where a, b, and c are fitted constants, and n represents the charge transfer n_{ad}.[22] The $1/\rho$ behavior begins when $\rho \geq 0.04$ for all AMs except Li, for which it begins when $\rho \geq 0.08$. This difference can be attributed to the small ionic radius of Li that affects the onset of depolarization fields to the dipole moment at the adatom-graphene interface.

As ρ increased, d_{eff} showed a strong coverage dependence as n_{ad} and n_c [Fig. 3(a)]. For all AMs, d_{eff} was minimal at when $\rho \approx 0.04$ adatom/C, except for Li, for which the minimum occurred at $\rho \approx 0.08$ adatom/C. Interestingly, not only d_{eff} shows a dip at the same $\rho \approx 0.04$ adatom/C (except for Li) but also it falls into almost a single curve. This indicates that the behavior has some electronic origins as discussed below. The overall trend is explained by two factors: the strengthening of ionic bonding as ρ increases up to 0.04 (0.08 for Li) and increase in the ionic radii due to less charge transfer when $\rho > 0.04$ (0.08 for Li). At low coverage ($\rho < 0.04$), the increase in ρ enhances the Coulomb attraction and thus reduces the binding distance because whole one electron transfers from AM to graphene. When $\rho > 0.04$, the charge transfer decreases from one and the ionic radii of (fractionally charged) AM increase. Therefore, the increase in binding distance for $\rho > 0.04$ (0.08 for Li) is almost all due to the increase in the size of AM. The change of the graphene-adadom layer distance may not be observed in graphite intercalation due to the strong constraining force of graphite layers.

W was calculated with the vacuum level set to the saturated electrostatic potential in the region far from graphene [Fig. 3(b)]. In the supercell calculations, the graphene-adatom layers form an infinite series of dipole layers, which generate nonsaturating electrostatic potential even in the

middle of the supercells. To cancel such artificial dipole fields in the far region, we double the supercell size to put two graphene-adatom layers in a cell with inverting graphene-adatom sequence of the second layer from the first one. Two factors contribute to the work-function shift (ΔW): the Fermi level shift from the Dirac point due to charge transfer, and the dipole field by adatom-graphene layer. The dipole field effect can be modeled using the Helmholtz equation $\Delta W = -4\pi pN$, where N $(=g\rho$ with $g=3.78 \times 10^{14}$ carbon/cm^2) is the number of adatoms per unit area and p is the dipole moment perpendicular to the graphene surface.[23] This equation describes the linear dependence of ΔW on the number of adatoms at low coverage. When the density of adatoms increases above certain coverage or the interadatom distance becomes shorter than the screening length, each dipole feels the depolarization field E_d due to the adjacent dipoles. Assuming the adlayer to be uniform and ordered, $E_d = 8.89N^{3/2}p$,[24] and the dipole moment of a single adatom can be expressed as $p = p_0 - \alpha E_d$, where α is the polarizability. By substitution, $\Delta W = \frac{4\pi p_0 N}{1+8.89\alpha N^{3/2}}$ (Ref. 25) and is minimum at the density $N_0 = (\frac{2}{8.89\alpha})^{3/2}$. This depolarization effect was not observed in the graphene layer side, which instead showed a saturating behavior as ρ increased. Previous studies showed such a saturating behavior in AM-adsorbed graphite, but not a dip in ΔW.[26] This asymmetric behavior of the work function shift may be observed in suspended graphene.

The ionic radius of Li is smaller than that of other AMs, and this explains why the onset of the depolarization field effect begins at higher ρ for Li than that for other AMs. The energy window in the planar charge distribution of the states in the energy range from −0.9 eV up to the Fermi level at the $2\times 2R0°$ phase [Fig. 4(a)] corresponds to the occupied state due to electrons transferred from the adatom. A rather uniform charge density occurred around K atoms, but Li experiences the corrugation in the carbon hexagons of graphene. Figure 4(b) shows the averaged electrostatic potential of pristine graphene that each adatom may feel at its binding site. Li atoms experience a stronger potential than other AMs due to its small ionic radius, and other AMs feel almost the same potential as each other. This result is also consistent with previous calculations of the diffusion barrier for AMs from one stable binding site to another over carbon bridges,[20] which showed a relatively large barrier for Li (~0.2 eV) but almost barrierless for other AMs. Relatively tightly bound electrons near Li adsorption sites screen the dipole moment more effectively than in other AMs, and this causes depolarization to begin at higher ρ for Li than for other AMs. The size of carbon hexagon ring is a gauge to differentiate the small and the large ionic radii that feel the corrugation and to determine when depolarization comes into effect. To test this idea that ionic radii affect metallic interaction, we artificially increased the C-C bond length as if external (isotropic) strain were applied, then repeated the same calculation for Na; the crossover coverage is shifted from $\rho \approx 0.04$ to $\rho \approx 0.07$ (adatom/C) at about 10% strain and d_{eff} also decreased.

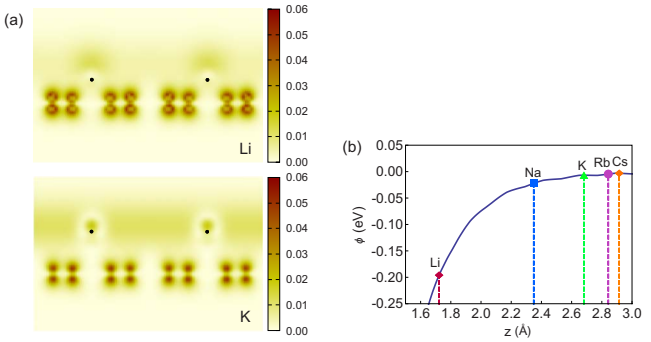

FIG. 4. (Color online) (a) The plot in a plane perpendicular to graphene of charge density contributed by the states lying within the energy range from −0.9 eV up to the Fermi level in graphene with $2\times 2R0°$ adatom phase. Upper panel: Li; lower panel: K. Black dots indicate the position of adatoms. The scale bar has units of electron/Å^3. Li was more closely bound to graphene than were all other AMs (here only K is shown) that show a more uniform charge density compared to Li. (b) The electrostatic potential (ϕ) of pristine graphene that should affect adatoms at their binding positions. This shows that Li will experience a significantly stronger potential than other AMs.

SUMMARY

The adsorption of AMs on graphene was studied using first principles calculations. We observed a crossover in characteristic properties such as binding distance, charge transfer, and work function as adsorbed AMs change characters from isolated AM atoms at low ρ to metallic sheets at higher ρ. The minima occurred at almost the same ρ for all AMs except Li; the differences in results were attributed to differences in the ionic radii. The size of the carbon hexagon ring is the gauge that distinguishes the difference in the ionic radii. For all AMs, a minimum in the calculated ΔW of graphene occurred at the same ρ as the other characteristics; this behavior is attributed to the depolarization effect as adatoms form 2D metallic sheet.

ACKNOWLEDGMENTS

S.-H.J. thanks J.-S. Kim for helpful discussion. This research was supported by the National Research Foundation of Korea funded by the Ministry of Education, Science and Technology (Grant No. 2009-0087731 and WCU Program No. R31-2008-000-10059-0).

*Corresponding author; jhish@postech.ac.kr

[1] K. S. Novoselov, A. K. Geim, S. V. Morozov, D. Jiang, M. I. Katsnelson, I. V. Grigorieva, S. V. Dubonos, and A. A. Firsov, Nature (London) **438**, 197 (2005).
[2] Y. Zhang, Y.-W. Tan, H. L. Stormer, and P. Kim, Nature (London) **438**, 201 (2005).
[3] A. H. C. Neto, F. Guinea, N. M. R. Peres, K. S. Novoselov, and A. K. Geim, Rev. Mod. Phys. **81**, 109 (2009).
[4] A. K. Geim and K. S. Novoselov, Nature Mater. **6**, 183 (2007).
[5] N. Park, S. Hong, G. Kim, and S.-H. Jhi, J. Am. Chem. Soc. **129**, 8999 (2007).
[6] T. Ohta, A. Bostwick, T. Seyller, K. Horn, and E. Rotenberg, Science **313**, 951 (2006).
[7] Jannik C. Meyer, A. K. Geim, M. I. Katsnelson, K. S. Novoselov, T. J. Booth, and S. Roth, Nature (London) **446**, 60 (2007).
[8] A. Bostwick, T. Ohta, T. Seyller, K. Horn, and E. Rotenberg, Nat. Phys. **3**, 36 (2007).
[9] S.-M. Choi and S.-H. Jhi, Phys. Rev. Lett. **101**, 266105 (2008).
[10] C. G. Hwang, S. Y. Shin, S.-M. Choi, N. D. Kim, S. H. Uhm, H. S. Kim, C. C. Hwang, D. Y. Noh, S.-H. Jhi, and J. W. Chung, Phys. Rev. B **79**, 115439 (2009).
[11] M. S. Dresselhaus and G. Dresselhaus, Adv. Phys. **30**, 139 (1981).
[12] M. S. Dresselhaus, G. Dresselhaus, J. E. Fischer, and M. J. Moran, *Intercalated Graphite*, Material Research Symposium Series (North-Holland, New York, 1983), Vol. 20.
[13] D. P. DiVincenzo and E. J. Mele, Phys. Rev. B **32**, 2538 (1985).
[14] J. P. Perdew and A. Zunger, Phys. Rev. B **23**, 5048 (1981).
[15] G. Kresse and J. Hafner, Phys. Rev. B **47**, 558 (1993).
[16] D. M. Ceperley and B. J. Alder, Phys. Rev. Lett. **45**, 566 (1980).
[17] P. A. Khomyakov, G. Giovannetti, P. C. Rusu, G. Brocks, J. van den Brink, and P. J. Kelly, Phys. Rev. B **79**, 195425 (2009).
[18] C. Kittel, *Introduction to Solid State Physics* (Wiley, New York, 1996).
[19] M. Caragiu and S. Finberg, J. Phys.: Condens. Matter **17**, R995 (2005).
[20] K. Rytkönen, J. Akola, and M. Manninen, Phys. Rev. B **75**, 075401 (2007).
[21] K. T. Chan, J. B. Neaton, and M. L. Cohen, Phys. Rev. B **77**, 235430 (2008).
[22] S. M. Choi and S. H. Jhi, Appl. Phys. Lett. **94**, 153108 (2009).
[23] G. A. Somorjai, *Introduction to Surface Chemistry and Catalysis* (Wiley, New York, 1994).
[24] J. Topping, Proc. R. Soc. London, Ser. A **114**, 67 (1927).
[25] B. L. Maschhoff and J. P. Cowin, J. Chem. Phys. **101**, 8138 (1994).
[26] A. Natori, T. Ohno, and A. Oshiyama, J. Phys. Soc. Jpn. **54**, 3042 (1985).